

LA-UR-96-1371

CONF-960804-31

Title:

ENVIRONMENTAL WASTE SITE
CHARACTERIZATION UTILIZING AERIAL
PHOTOGRAPHS, REMOTE SENSING, AND SURFACE
GEOPHYSICS

Author(s):

RECEIVED

MAY 3 1 1996

Ed Van Beekhout, Paul A. Pope, EES-3
Cheryl Rofcr, Scott Baldrige, EES-1
John Ferguson, Univ. of Texas
George Jiracek, San Diego State University
Lee Balick, Bechtel Remote Lab.
Nick Josten and Mike Carpenter, Idaho
National Eng. Lab.

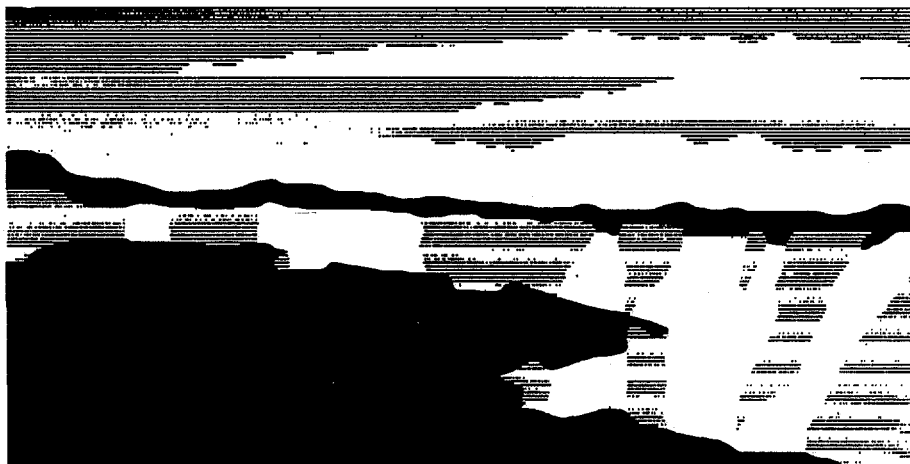
OSTI

Submitted to:

Nuclear and Hazardous Waste Management
International Meeting: SPECTRUM August 19-23,
1996

MASTER

Los Alamos
NATIONAL LABORATORY



Los Alamos National Laboratory, an affirmative action/equal opportunity employer, is operated by the University of California for the U.S. Department of Energy under contract W 7405 ENG 36. By acceptance of this article, the publisher recognizes that the U.S. Government retains a nonexclusive, royalty-free license to publish or reproduce the published form of this contribution, or to allow others to do so, for U.S. Government purposes. The Los Alamos National Laboratory requests that the publisher identify this article as work performed under the auspices of the U.S. Department of Energy.

Form No. 836 R6
ST 2629 10/91

DISTRIBUTION OF THIS DOCUMENT IS UNLIMITED

cc

DISCLAIMER

**Portions of this document may be illegible
in electronic image products. Images are
produced from the best available original
document.**

ENVIRONMENTAL WASTE SITE CHARACTERIZATION UTILIZING AERIAL PHOTOGRAPHS, REMOTE SENSING, AND SURFACE GEOPHYSICS

Paul Pope, Ed Van Eeckhout, Cheryl Rofer, and Scott Baldrige
Los Alamos National Laboratory, Los Alamos, NM 87545 (e-mail: emvan@lanl.gov)

John Ferguson

University of Texas at Dallas, Richardson, TX 75080

George Jiracek

San Diego State University, San Diego, CA 92182

Lee Balick

Bechtel Remote Sensing Laboratory, Nellis Air Force Base, Las Vegas, NV 89193-8521

Nick Josten and Mike Carpenter

Idaho National Engineering Laboratory, Idaho Falls, ID 83415-2107

ABSTRACT

Six different techniques were used to delineate a 40 year old trench boundary at Los Alamos National Laboratory. Data from historical aerial photographs, a magnetic gradient survey, airborne multispectral and thermal infra-red imagery, seismic refraction, DC resistivity, and total field magnetometry were utilized in this process. Each data set indicated a southern and northern edge for the trench. Average locations and 95 percent confidence limits for each edge were determined along a survey line perpendicular to the trench. Trench edge locations were fairly consistent among all six techniques. Results from a modeling effort performed with the total magnetic field data was the least consistent. However, each method provided unique and complementary information, and the integration of all this information led to a more complete characterization of the trench boundaries and contents.

I. INTRODUCTION

The Los Alamos National Laboratory (LANL), located in northern New Mexico (Fig. 1), has been engaged in cleaning up many of its old hazardous waste sites for a number of years. Past records, current and historical aerial photographs, satellite and airborne remote sensing, as well as geophysical surveys have all been used to characterize waste sites. The effective combination of these data has provided clear insight into defining problem areas, as well as indicating where more detailed information might be required.¹

Historical aerial photography, remote sensing, and surface geophysics all supply non-intrusive data about the physical parameters of a waste site, from which the necessary characterization information may be derived. The usefulness of historical aerial photographs characterizing waste sites is well documented.^{2,3,4,5} The use of remote sensing data for waste site characterizations is extremely varied and is

receiving increased interest from the scientific community. Multispectral (reflective) and thermal (emissive) imagery can provide information about disturbed ground, vegetation stress, buried waste locations, soil moisture, and subsidence.^{6,7,8,9} Surface geophysics are routinely used for characterizing waste sites.¹⁰ For example, ground Penetrating Radar (GPR), thermography, and total field magnetometry can be used to determine the location and depth of buried objects at hazardous waste sites.^{11,12} No single technique is a "silver bullet" which can provide all the information necessary for characterizing a site. Combinations of remotely sensed and geophysical

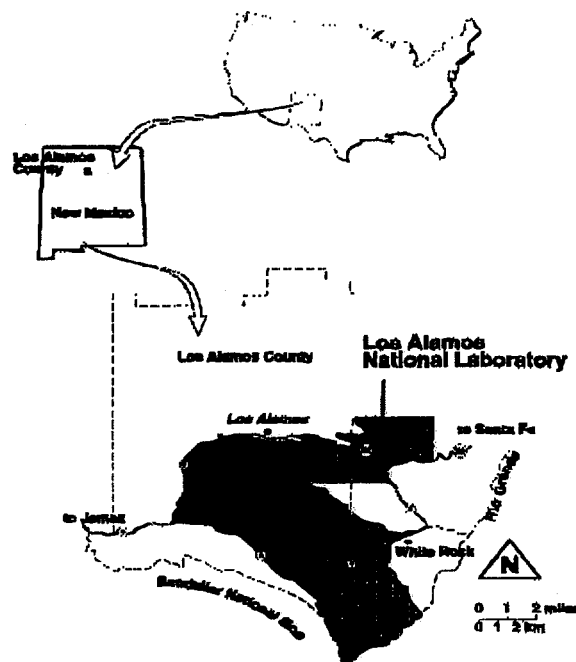


Fig. 1. Location map of Los Alamos National Laboratory.

data, along with a variety of other data, can provide a more thorough site description. A Geographic Information System (GIS) is particularly adept at storing and combining spatial data from disparate sources to aid in this process.¹³

II. STUDY SITE

The Los Alamos National Laboratory lies on the Pajarito Plateau on the eastern side of the Jemez mountains at an average elevation of 7,500 ft. The environment of the region is characterized as semi-arid (high desert). The plateau is comprised of a series of narrow mesas and canyons. The mesas of the Pajarito Plateau are composed primarily of Bandelier Tuff, a series of ash-flow deposits that were formed 1.1 to 1.5 million years ago. The tuff is soft and easily workable with power equipment. Soil cover on the mesa tops is typically less than 4 ft deep. The waste site for this work is known as Materials Disposal Area F (MDA-F) and is located on the northern edge of one of the mesas in the region (Fig. 2).



Fig. 2. Material Disposal Site F as it appears today.

MDA-F was used during World War II for explosives testing and detonation of high explosive lenses. After the war, the area was used for trench burial of test-related, obsolete materials. The trenches were excavated through the top soil and into the tuff, and then backfilled and capped with crushed tuff and soil. The area has been reclaimed by Ponderosa Pine and herbaceous vegetation. It is possible that high explosives may have been buried in the trenches. Therefore, it is important to identify and delineate the boundaries of the trenches in the area so that intrusive sampling can be performed near the disposals without intercepting the waste. The main burial trench at MDA-F was chosen for this study because it probably contains the bulk of the buried waste and is the largest of the four trenches at the site.

III. METHODOLOGY

The data sets used in this study have been gathered by different organizations, at different times, and for

different reasons. Therefore, the actual integration of data was not performed in serial, but iterative fashion. Results from one method often required others be revisited. These data represent two different views of the site: a planar view (photography, remote sensing, and magnetic gradient) and a cross-sectional view (seismics, DC resistivity, and total field magnetometry). These data were of differing quality and coverage area. Therefore, a survey line within the region of overlap was used to integrate the data and aid in comparison of results.

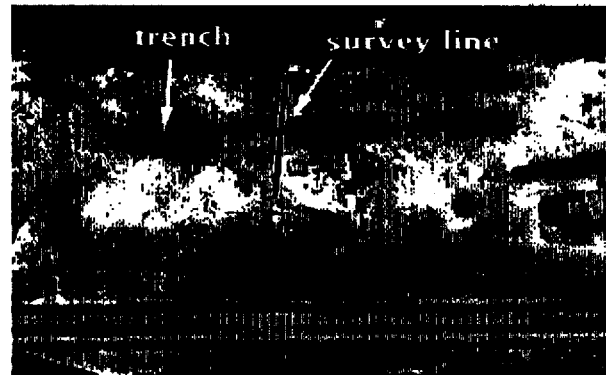


Fig. 3. The survey line overlaid on 1958 photograph of MDA-F.

The survey line used was defined approximately perpendicular to the edges of the trench (Fig. 3). The north and south edges of the main east-west trench marked in Fig. 3 were the target for this study. For each data set the location of the southern and northern trench edges are expressed as distances from the southern stake along the survey line. For simplicity the derivation of the trench edges along the survey line was treated as a one-dimensional problem. That is, location errors perpendicular to this line were not addressed.

The location error for the historical photography, remote sensing, and magnetic gradient techniques comes from two sources. First, the georeferencing of the data incurs some error. The second source is from measurement error. The measurement error depends, in part, on the sampling resolution (spatial resolution) of each technique. A conservative estimate of the total error for each of these techniques was obtained by adding the georeferencing and measurement errors. The location error for the other geophysical surveys is due to measurement error only, since these surveys were deployed directly along the survey line.

A. Historical Aerial Photography

Historical aerial photographs were analyzed to provide a physical history and preliminary mapping

information for characterizing the site.¹⁴ Photographs were digitized by scanning. Digital analysis of these photographs allowed disparate views of the waste site to be transformed so that they matched a base image in scale, orientation, and extent. This was especially useful for oblique photographs of the waste site. The coregistered images were studied individually and collectively to identify features which were indicative of human activity at the site and to provide a physical history of natural and human induced changes. The coregistered images were imported to a GIS and georeferenced to a 1991 base image. Boundaries of features such as suspected trenches and disturbed soil were extracted by on-screen digitizing.

The base image used for georeferencing of the historical aerial photographs was a digital mosaic of two orthophotographs of the waste site. These photographs were taken in 1991 at a scale of 1:1,200. The base image was georeferenced to NMCS coordinates with an accuracy of 2.6 ft. The georeferencing accuracy of an image which is transformed to match this base image can be no better than 2.6 ft, and was conservatively estimated by adding this error to the error incurred in the transformation process.

Vertical aerial photographs from a 1958 survey at 1:50,000 scale showed the trenches with the greatest clarity and with the highest accuracy of all the historical photographs (Fig. 3). The trenches appeared as dark rectangles with very bright, disturbed ground around them. The dark appearance of the trenches was probably due to forbs which were growing on the refill material. This image was rectified to match the base image by using an affine transformation and nearest neighbor resampling. The accuracy of the rectification was 3.3 ft. The total georeferencing accuracy was estimated to be 3.3 ft plus 2.6 ft, or 5.9 ft.

The extent of the forb regrowth was vectorized by manual on-screen digitization. These boundaries were assumed to represent the trench edges. Even though the spatial resolution of this image was high (0.3 ft per pixel), the boundaries of these features were not well defined. The measurement accuracy of this visual interpretation was estimated to be 3.3 ft. The survey line vector and the main trench boundary were intersected so that the locations of the trench edges along this line could be determined. The southern and northern trench edges as measured along the survey line from the southern stake were 48.2 ft and 77.4 ft, respectively. The error of these locations was estimated as the sum of the georeference and measurement errors, or 9.2 ft.

B. Remote Sensing

The DOE Remote Sensing Laboratory, located at Nellis AFB Nevada and managed by Bechtel, used a Daedalus AADS 1268 Multispectral Scanner to collect imagery over LANL in June of 1994. The imagery consisted of both daytime multispectral and pre-dawn thermal IR acquisitions at a spatial resolution of 3.3 ft per pixel.¹⁵ The imagery was imported to the GIS and georeferenced by using the 1991 orthophoto mosaic as the base image. An affine transformation and nearest neighbor resampling was used. The accuracy of this transformation was 3.3 ft. The total error in georeferencing this imagery was estimated by adding the transformation error to the georeferencing error of the base image, or 5.9 ft.

The daytime multispectral imagery included five bands which corresponded to reflected wavelengths of energy (0.45 to 2.35 microns). The correlation between all pairs of reflected wavelength bands was calculated. The three bands with the least correlation were used to create false color images. The five bands of imagery were also used as input to a principal components analysis. Another false color image was created by using the first three principal component bands.

The survey line was overlaid on these images and visually inspected. Neither false color image was able to provide information about the trench locations along the survey line. The land cover over the trenches is very similar to the surrounding land cover, so the boundary between the two was not easily distinguished. However, disturbed ground around the trenches from past activity and more recent disturbances was enhanced. An old access road, not easily detectable on the ground nor from recent color aerial photography, was easily distinguished in both of the false color images. The extent of this disturbed ground matched the general extent noted in the 1958 aerial photo. However, an exact comparison was hampered due to the Ponderosa Pine which cover the site.

The pre-dawn thermal imagery was also analyzed. The thermal image was linearly enhanced and the survey line was overlaid. A thermal anomaly was visible at the location of the survey line and was assumed to correlate with the main trench. This anomaly had a cooler brightness temperature than the surrounding area. The north and south edges of the thermal anomaly were digitized as points along the survey line. These positions were then transformed from NMCS coordinates to distances from the southern stake along the survey line. The locations of the southern and northern trench edges were 47.9 ft

and 89.9 ft, respectively. The measurement error of this visual interpretation was estimated to be 3.3 ft. The error of these locations was estimated by adding the georeferencing and measurement errors, or 9.2 ft.

C. Magnetic Gradient Survey

The Idaho National Engineering Laboratory (INEL) used an innovative instrument called the Rapid Geophysical Surveyor (RGS) to perform a magnetic gradient survey over a portion of MDA-F.¹⁶ The RGS recorded magnetic gradient data, in units of nanoTesla per meter, for the vertical component of the magnetic field over the waste site. The magnetic field over the site is influenced by ferrous materials either lying on the surface or buried at various depths. The RGS was used to collect magnetic data over a 212 by 596 foot area. The corners of this area were surveyed to determine their NMCSF coordinates. The RGS was pushed along survey lines in a south to north direction. This process was then repeated by surveying from north to south. The data was reduced to an evenly spaced, gridded set with a 1 foot interval, which created an image of magnetic anomalies at the site. Analysis of spatial patterns and trends in this image was used to derive seven different anomaly areas. Profiles through the data revealed several magnetic signatures which were repeated at various locations. These signatures helped to interpret the shape, orientation, depth, and size of the ferromagnetic objects.

The image was imported to the GIS and georeferenced. The image was georeferenced by using the NMCSF coordinates of the four corners of the survey area. An affine transformation and nearest neighbor resampling were used. The location accuracy of the surveyed corner locations was 1.0 foot. The accuracy of the transformation was also 1.0 foot. The total georeferencing error was estimated by adding these errors, or 2.0 ft. The survey line vector was used to extract a profile of the magnetic gradient values from the image. The trench edges were identified as two small amplitude rises in the profile. The midsection of this profile, in between the two rises, contained large amplitude fluctuations due to numerous pieces of ferromagnetic material within the trench boundary. The location of the trench edges were assumed to be the peaks of the two small rises. The southern and northern trench edges relative to the southern stake were 81.0 and 44.0 ft, respectively. The measurement error was estimated to be one half of the one foot sampling interval. The location error was estimated to be the sum of the georeferencing and measurement errors, or 2.5 ft.

D. Other Geophysical Methods

The Summer of Applied Geophysical Experience (SAGE) is an intensive three week student program which concentrates on the theory and hands-on application of current geophysical technology to geological and environmental problems.¹⁷ The students and faculty of the SAGE '95 program had the opportunity to conduct various geophysical measurements of the main trench at MDA-F on June 27 and 28. Three different techniques were used to determine the location, dimensions, and contents of the trench. The techniques used were seismics, DC resistivity, and magnetics.

The geophysical data gathered by these three methods were processed to determine the location of the north and south trench edges relative to the southern stake position. Information about the width and depth of the trench were also derived, as well as qualitative information about its contents. These surveys were deployed in the field along the survey line. The edge locations were expressed as distances along this line relative to the southern end. Therefore, georeferencing error was not included in the assessment of the location error. The location error was assumed to equal the measurement error.

1. Seismic Refraction

Seismic recordings were taken along three lines. Each line was 141 ft long and contained 48 geophones spaced 3.0 ft apart. Eight shot points were placed along each survey line. They were spaced 18 ft apart, and placed halfway between the two nearest geophones. Each line was started with a shot point 1.5 ft beyond the first geophone. A hammer was used as a seismic wave source at each shot point. Twelve shots were made at each location and the signals from the geophones were recorded by a seismogram. The twelve records were stacked to reduce signal noise and form one record for each shot point. Two lines, isolated from any obvious excavation, were shot for velocity control. The third line was shot across the trench.

A two layer, infinite half-space model was assumed. The first layer was the top soil and trench fill material and the second layer was the surrounding Bandelier Tuff. The soil and trench fill were assumed to have about the same seismic velocity. First arrival time picks were difficult due to the noise encountered on the furthest six geophones from the shot point. Travel time curves were plotted for each of the shot points along the survey line. The trench edges were seen as distinct changes in the slope of the travel time curves. The velocity inside the trench was faster than the surrounding tuff. The travel times

were processed using a program called SIPT2.¹⁸ This program attempts to define topography on a refracting interface using time delays and ray tracing in an automatic manner. Early results using this code were encouraging, however, closer inspection revealed that the models produced by this process were inadequate.

A very flexible system was devised for models specified as polygonal prisms.¹⁹ Any number of layers or bodies can be specified, each one having an N-sided polygonal outline. A velocity function is specified for each polygon. This specification is very convenient for interpretation, but not for computation. The travel times are computed by rasterizing the velocity distribution onto a grid. The travel times are then computed using a finite difference wavefront extrapolation code. A second generation wavefront extrapolation code is used, which has none of the limitations of the early Vidale (1988) method.^{20,21} This code is used to model in the forward sense only. Models are defined a priori and the results evaluated. The model is not automatically redefined. This permitted the testing of some very simple hypotheses about the excavations, which could not be evaluated by the Rimrock software or simple flat layered models.

It was possible to constrain the width of the trench very accurately by inspection of the travel time curves. The error in the measurement of the total width of the trench is approximately equal to one geophone interval, or 3.0 ft. The two velocity control lines determined the tuff and soil velocities to be 2900 ft per sec and 750 ft per sec, respectively. The average soil depth was estimated to be about two ft. The trench was modeled as a vertical sided rectangle, overlain by soil. The fill material is characterized by a velocity of 1200 to 1300 ft per sec. The depth was estimated to be 18 ft with an accuracy of 3.3 ft. This is about twice the depth determined from the earlier models. The difference is due in part to the recognition that the velocity of the fill material is faster than the soil by almost a factor of two.

It became clear in the modeling that the arrivals on the far side of the trench from the shot point were shadowed by the trench and had a very poor signal to noise ratio. This had caused false identifications of later arriving energy as the initial P-wave. These records were repicked, but in some cases the true first arrivals were simply lost in the noise. These falsely identified arrivals had a very deleterious effect on the SIPT2 delay time based models. Critically refracted waves, propagating up the vertical side of the pit, on the far side from the shot point, are identified. These unusual arrivals are very sensitive to the pit depth. Some indications of asymmetry in the trench

geometry have not been pursued at this time. It would be instructive to rerun the SIPT2 processing with the improved time picks and velocity information.

The model implies a rectangular pit 30 ft wide and 18 ft deep. Inspection of the modeled cross section of the trench shape provided information about the location of the trench edges. The northern and southern trench edges relative to the southern stake position were 47.9 ft and 89.9 ft, respectively. The error in these locations was estimated to be one geophone interval (3.0 ft).

2. DC Resistivity

Apparent resistivity measurements were taken with a transmitter and receiver interval of 3.3 ft (1 meter) in a dipole-dipole configuration. The distance between the transmitter and receiver dipoles was changed in 3.3 foot intervals. The relative positioning of transmitter and receiver was varied along the survey line in the following manner. The transmitter dipole was placed so that its midpoint was over the southern stake. The receiver dipole was placed so that its midpoint was two meters away from the midpoint of the transmitter. A geometric factor was used to index the position of the receiver. The first position was given an index of one. A DC electric current of less than half an ampere was passed into the ground by the transmitter. The voltage across the poles of the receiver was measured. Apparent resistivity, in units of ohm meters, was calculated by dividing the receiver voltage by the transmitter current and multiplying by the geometric factor. The receiver dipole was moved so that its midpoint was three meters away from the midpoint of the transmitter. The geometric factor was changed to a value of two. Electric current was passed through the ground again. The voltage was measured at the receiver, and an apparent resistivity was calculated. This process was repeated until the receiver dipole had been moved six more times. Therefore, the geometric factor was varied from one to eight. The midpoint of the transmitter dipole was then moved 3.3 ft along the survey line and the process was repeated. A total of 23 transmitter positions and eight receiver positions per transmitter position were used.

A pseudo-section of the apparent resistivity measured by varying the relative positioning of the transmitter and receiver dipoles was made. A contour plot of apparent resistivity was created from this pseudo-section. The trench edges were indicated by distinct divergences of the contour lines, called "pants legs" at the top of the plot (ground surface). This effect is caused by a build up of charge (galvanic effect) at the interface of the trench fill and the surrounding

Bandelier Tuff. The contour plot also indicated that the trench is resistive overall with a central resistivity of 140 ohm meters and an average value of 65 ohm meters. The center positions of the "pants legs" in the pseudo-section plot were assumed to represent the locations of the trench edges. The northern and southern trench edges relative to the southern stake were 50.2 ft and 77.1 ft respectively. The location error was estimated to be one half of the dipole interval (1.7 ft).

3. Total Field Magnetometry

A proton precession magnetometer was used to measure the total magnetic field strength along the survey line. The magnetic strength was measured in units of nanoTeslas by traversing the survey line in 1.6 foot (0.5 meter) intervals. A magnetic signature was created by graphing the field strength versus the position along the survey line.

The trench was modeled as a metallic, rectangular prism anomaly with an east-west strike.²² This model expresses the total magnetic field as a function of the width of the body, depth from the surface to the top of the body, depth from the surface to the bottom of the body, and the center position of the body. Constants in the model were the polarization direction, the magnetic susceptibility, and the inclination of the local magnetic field. The regional magnetic trend was assumed to be linear and was removed from the data by forcing the two end points of the magnetic signature to touch the zero line of the graph. The variables in the model were changed until the calculated signature matched the measured signature as closely as possible. The fit was determined subjectively.

The results of the modeling were an anomaly width of 18.4 ft, 5.3 ft from the surface to the top, 23.6 ft from the surface to the bottom, and a center position of 72.2 ft away from the southern stake. The location of the southern trench edge was calculated as half the width subtracted from the center position, or 63.0 ft. The location of the northern trench edge was calculated as half the width added to the center position, or 81.4 ft. The location error was estimated to be 6.6 ft. This estimate was derived from a sensitivity analysis of the mathematical model.

Further analysis lead to the conclusion that the edge locations derived from modeling of the total magnetic field measurements were probably very unreliable. Evidence against the model used in this analysis was provided by the magnetic gradient and DC resistivity surveys. These surveys did not support the assumption of a solid mass of metal buried at depth. They implied an abundance of refill material with

some ferromagnetic objects dispersed within the trench. Therefore, the locations derived from the modeling of the total field magnetometry data was excluded from the rest of the analysis.

IV. SYNTHESIS

The location of the northern and southern trench edges as determined from all six techniques are summarized in Table 1 and visually in Fig. 4. Best estimates for the edge locations and 95 percent confidence intervals for these positions were sought. The statistics for this analysis were difficult to evaluate due to a lack of numerous samples of the edge locations for each technique. Assumptions were made about the distribution of the mean trench edge locations. The population of all possible mean locations for a particular edge was assumed to be normally distributed. The mean of this distribution was assumed to be equal to the average of the locations derived from each technique. The variance was assumed to be dependent on the variances due to differences between the techniques and differences in the measurement errors for each method.



Fig. 4. Data results overlaid on 1958 image of the site. Measurements are in ft.

The best estimates of the trench edge locations were derived by taking the average of the locations for each edge. The mean location of the southern edge is 47.6 ft with a standard deviation of 2.2 ft. The mean location of the northern edge is 83.1 ft with a standard deviation of 6.4 ft. This suggests a width of 35.5 ft. It was assumed that the variance of these positions comes from two sources. The first is the variance between techniques. This was estimated by squaring the standard deviations of the best estimates, which yields 4.8 ft² for the southern edge

and 41.0 ft² for the northern edge. The second source is the total variance due to the different measurement errors for each technique. The total measurement error variance was estimated as the average of the individual measurement variances, or 30.4 ft². The

total variances were calculated as the sum of the variances attributed to differences in technique and measurement error, or 35.2 ft² for the southern edge and 71.4 ft² for the northern edge.

Table 1. Summary of the Trench Edge Locations and Errors

Technique	Southern Edge [ft]	Northern Edge [ft]	Location Error [ft]
Historical Aerial Photography (1958 photograph)	48.2	77.4	9.2
Remote Sensing (Predawn thermal image)	47.9	89.9	6.6
Magnetic Gradient Survey	44.0	81.0	2.0
Seismic Refraction	47.9	89.9	3.0
DC Resistivity	50.2	77.1	3.3
Total Field Magnetometry (rectangular, vertical prism model)	63.0	81.4	6.6

The 95 percent confidence interval depends on the standard error of the best estimate locations. The standard error of the best estimate locations was derived by dividing the total variances for these positions by five (the number of data sets) and taking the square root. The standard errors were 2.6 ft and 3.8 ft for the southern and northern edges, respectively. The standard errors were multiplied by a Student's t-value of 2.776 (4 degrees of freedom) to calculate the half widths of the 95 percent confidence intervals. These half widths were 7.2 ft for the southern edge and 10.5 ft for the northern edge. These values were added and subtracted to the associated mean edge locations to form the 95 percent confidence intervals. The interval for the southern edge is 40.4 ft to 54.8 ft, and 72.6 ft to 93.6 ft for the northern edge. The best estimates for the edge locations and the 95 percent confidence intervals are shown in Figure 4.

The trench edges delineated from each data set were fairly consistent. The results from the modeling effort performed with the total magnetic field data were the least consistent. The southern edge of the trench appears less well resolved than the northern edge. It is unclear what is causing this effect. The historical aerial photography and remote sensing (thermal infrared) imagery generally have a higher location error than the geophysical data sets. The lower accuracy was caused by the propagation of errors encountered in georeferencing these data as well as the general lack of detail in these images. The edge locations from the DC resistivity analysis seem to suggest a smaller width than the other techniques. The edge locations from the pre-dawn thermal imagery and the modeling analysis of the seismic data seem to be very consistent. The 95 percent confidence intervals are reasonable given the

variances between techniques and the differences in measurement error for each method.

V. CONCLUSION

All six data sets indicated the existence of the main trench in unique and complementary ways. The historical aerial photographs and remotely sensed imagery provided an overall view of the site and identified where more detailed and labor intensive geophysical surveys should be deployed. The trench was identified as a dark, rectangular patch of anomalous vegetation in the historical aerial photography. The pre-dawn thermal imagery indicated a cooler brightness temperature for the trench. The refraction technique provided the best information about the depth of the trench, while the magnetic gradient and DC resistivity techniques provided the best qualitative information about its contents. The analysis of the seismic refraction data estimated the depth of the trench to be 18 ft. The model used to process the total field magnetometry data was probably inappropriate given the information from the magnetic gradient and DC resistivity surveys. Analyses of the magnetic gradient and DC resistivity data suggest that the trench contains numerous pieces of ferromagnetic material dispersed within a large amount of resistive refill material. The GIS was very useful for organizing and combining the spatial information from the various surveys.

This work was a limited attempt at integrating data from disparate sources. A more in-depth and rigorous study should be performed. Increased sampling of the trench edge by each technique should be attempted to support a more well defined statistical analysis. The increased sampling should be performed along the

same survey line. Alternatively, other survey lines could be used so that the edges of the trench are sampled over the entire length of the trench. This design might be useful for creating a map of the 95 percent confidence intervals around the trench. Data from other surface geophysical techniques would be useful, such as ground penetrating radar and transient electromagnetics.

ACKNOWLEDGMENTS

The assistance of all the SAGE '95 students, especially Meghan Miller, Cynthia Dawn Snow, and Patricia Teston, is duly recognized. Conversations with Dr. Erik Nordheim (University of Wisconsin - Madison) were helpful in evaluating the statistics used in this research.

REFERENCES

1. Albers, B. J., C. Purdy, and D. F. Roelant, "Geomatics for Environmental Characterization and Monitoring within the Department of Energy (DOE)," presented at the Ninth Thematic Conference on Geologic Remote Sensing, Pasadena, California, Environmental Research Institute of Michigan, Ann Arbor, Michigan (1993).
2. Erb, T. L., W. R. Philipson, W. L. Teng, and F. Liang, "Analysis of Landfills with Historic Airphotos," *Photogrammetric Engineering and Remote Sensing*, Vol. 47, No. 9, pp. 1363-1369 (1981).
3. Lyon, J. G., "Use of Maps, Aerial Photographs, and other Remote Sensor Data for Practical Evaluations of Hazardous Waste Sites," *Photogrammetric Engineering and Remote Sensing*, Vol. 53, No. 5, pp. 515-519 (1987).
4. Airola, T. M. and D. S. Kosson, "Digital Analysis of Hazardous Waste Site Aerial Photographs," *Journal Water Pollution Control Federation*, Vol. 61, No. 2, pp. 180-183 (1989).
5. Sciacca, J. E., "Air Photo Interpretation for CERCLA and RCRA Investigations - A Technique That's Still Useful," *Proceedings: Ninth Thematic Conference on Geologic Remote Sensing, Pasadena, California*, pp. 97-110, Environmental Research Institute of Michigan, Ann Arbor, Michigan (1993).
6. Stohr, C., W. J. Su, P. B. DuMontelle, and R. A. Griffin, "Remote Sensing Investigations at a Hazardous-Waste Landfill," *Photogrammetric Engineering and Remote Sensing*, Vol. 53, No. 11, pp. 1555-1563 (1987).
7. Fenstermaker, L. K. and J. R. Miller, "Identification of Fluvially Redistributed Mill Tailings Using High Spectral Resolution Aircraft Data," *Photogrammetric Engineering and Remote Sensing*, Vol. 60, No. 8, pp. 989-995 (1994).
8. Herman, J. D., J. E. Waites, R. M. Ponitz, and P. Etzler, "A Temporal and Spatial Resolution Remote Sensing Study of a Michigan Superfund Site," *Photogrammetric Engineering and Remote Sensing*, Vol. 60, No. 8, pp. 1007-1017 (1994).
9. Stohr, C., R. G. Darmody, T. D. Frank, A. P. Elhance, R. Lunetta, D. Worthy, and K. O'Connor-Shoresman, "Classification of Depressions in Landfill Covers Using Uncalibrated Thermal-Infrared Imagery," *Photogrammetric Engineering and Remote Sensing*, Vol. 60, No. 8, pp. 1019-1028 (1994).
10. Daniel, D. E., *Geotechnical Practice for Waste Disposal*, pp. 311-357, Chapman and Hall, London, United Kingdom (1993).
11. Weil, G. J., R. J. Graf, and L. M. Forister, "Investigations of Hazardous Waste Sites Using Thermal IR and Ground Penetrating Radar," *Photogrammetric Engineering and Remote Sensing*, Vol. 60, No. 8, pp. 999-1005 (1994).
12. Foley, J. E., "Environmental Characterization with Magnetics and STOLS™," *Proceedings of the IEEE*, Vol. 82, No. 12, pp. 1823-1834 (1994).
13. Cowen, D. J., J. R. Jensen, P. J. Bresnahan, G. B. Ehler, D. Graves, X. Huang, C. Wiesner, and H. E. Mackey, Jr., "The Design and Implementation of an Integrated Geographic Information System for Environmental Applications," *Photogrammetric Engineering and Remote Sensing*, Vol. 61, No. 11, pp. 1393-1404 (1995).
14. Pope, P., E. Van Eeckhout, and C. Rofer, "Waste Site Characterization Through Digital Analysis of Historical Aerial Photographs," *Photogrammetric Engineering and Remote Sensing* (in press).
15. David, N. A., I. W. Ginsberg, E. M. Van Eeckhout, L. K. Balick, A. A. Lewis, J. B. Odenweller, G. A. Stahl, W. A. Tyler, and R. M. Weber, "Remote Sensing Characterization of Selected Waste Sites at the Los Alamos National Laboratory," Los Alamos National Laboratory report LAUR-95-3646, Los Alamos, New Mexico (1995).

16. Roybal, L. G., G. S. Carpenter, N. E. Josten, "Rapid Geophysical Surveyor," Proceedings of the Symposium on the Application of Geophysics to Engineering and Environmental Problems, April 18-22, San Diego, California, pp. 677-694, Environmental and Engineering Geophysical Society (1993).
17. Baldrige, W. S., and Jiracek, G. R., "SAGE Program explores the Rio Grande rift," *Eos, Transactions of the American Geophysical Union*, Vol. 73, pp. 145, 148-149 (1992).
18. Rimrock Geophysics, Inc., "User's Guide to SIPIT2 V-3.2", Lakewood, Colorado (1992).
19. Ferguson, J. F., A. H. Cogbill, and R. G. Warren, "A Geophysical-geological Transect of the Silent Canyon Caldera Complex, Pahute Mesa, Nevada," *J. Geophys. Res.*, Vol. 99, pp. 4323-4339 (1994).
20. Schneider, W. A., Jr., K. A. Ranzinger, A. H. Balch, and C. Kruse, "A Dynamic Programming Approach to First Arrival Traveltime Computation in Media with Arbitrary Distributed Velocities," *Geophys.*, Vol. 57, pp. 39-50 (1994).
21. Vidale, J., "Finite-Difference Calculation of Travel Times," *Bull. Seis. Soc. Am.*, Vol. 78, pp. 2062-2076 (1988).
22. Telford, W. M., L. P. Geldart, and R. E. Sheriff, *Applied Geophysics*, pp. 77,92-95, Second Edition, Cambridge University Press (1994).

DISCLAIMER

This report was prepared as an account of work sponsored by an agency of the United States Government. Neither the United States Government nor any agency thereof, nor any of their employees, makes any warranty, express or implied, or assumes any legal liability or responsibility for the accuracy, completeness, or usefulness of any information, apparatus, product, or process disclosed, or represents that its use would not infringe privately owned rights. Reference herein to any specific commercial product, process, or service by trade name, trademark, manufacturer, or otherwise does not necessarily constitute or imply its endorsement, recommendation, or favoring by the United States Government or any agency thereof. The views and opinions of authors expressed herein do not necessarily state or reflect those of the United States Government or any agency thereof.